Application of synthesized Mn_3O_4 nanoparicle in Mn_3O_4/H_2O_2 and $Mn_3O_4/H_3K_5O_{18}S_4$ processes for polyvinyl alcohol (PVA) removal from aqueous solution

Reza Shokoohi[a], Mohammad Taghi Samadi[a], Ghorban Asgari[a], Kazem Godini[b], Zahra Torkshavand[a], Mohammad Vanaei Tabar[a],*

[a]*Department of Environmental Health Engineering, Faculty of Health and Research Center for Health Sciences, Hamadan University of Medical Sciences, Hamadan, Iran, emails: m.vanaei1367@gmail.com (M.V. Tabar), reza.shokohi@umsha.ac.ir (R. Shokoohi), samadi@umsha.ac.ir (M.T. Samadi), g.asgari2003@gmail.com (G. Asgari), zahra.torkshavand@yahoo.com (Z. Torkshavand)*
[b]*Environmental Health Research Center, Research Institute for Health Development, Kurdistan University of Medical Sciences, Sanandaj, Iran, email: kgoodini@razi.tums.ac.ir (K. Godini)*

ABSTRACT

Polyvinyl alcohol (PVA) is one of the refractory chemicals that is widely used in several industries as raw material and may be released into receiving waters through unsanitary disposal of different wastewaters. This compound is considered as a hard biodegradable and resistant material and is harmful to human health. Its presence in water resources causes a disturbance in the deposition and removal of heavy metals and the formation of foam in water treatment processes. Therefore, in the current research, for the first time, we investigated the performances of Mn_3O_4/H_2O_2, $Mn_3O_4/H_3K_5O_{18}S_4$ methods in PVA removal from aqueous solutions. The effect of variables such as the concentration of peroxymonosulfate, hydrogen peroxide, Mn_3O_4 nanoparticle, PVA and contact time on the two processes were studied. Moreover, the analyses of X-ray diffraction, Brunauer–Emmett–Teller, Barrett–Joyner–Halenda, scanning electron microscopy, Fourier transform infrared spectroscopy and energy-dispersive X-ray spectroscopy were utilized to characterize the nanoparticles. The results showed that 93.14% and 67.98% of PVA was removed, respectively, by Mn_3O_4/H_2O_2 and $Mn_3O_4/H_3K_5O_{18}S_4$ under the following optimum conditions pH = 3, peroxymonosulfate concentration = 4.88 mmol/L, Mn_3O_4 concentration = 0.4 g/L, H_2O_2 concentration = 20 mmol/L and initial PVA concentration 100 mg/L.

Keywords: pH solution; Peroxymonosulfate; Nanoparticles; Co-precipitation method

1. Introduction

Polyvinyl Alcohol (PVA), which is generated from hydrolysis of polyvinyl acetate, is of refractory compounds in water and is widely applied in various industries such as textile, adhesives, paper, detergent, and so forth [1]. This compound is also used for the treatment of eye inflammation [2]. PVA is produced more than other water-soluble polymers [3]. Moreover, huge amounts of PVA are discharged into sewers, which can consequently be entered into the food chain and accumulates in the human body. It can also avoid heavy metals from sedimentation in rivers and lakes and this causes the metals to be distributed into the environment [4–7]. Therefore, the treatment of effluents containing PVA is of great importance. Common methods like electrocoagulation methods [2], biological degradation [2,8] and physical adsorption [9] cannot treat PVA efficiently. All these ways have their drawbacks such as high cost of operation and maintenance [10]. Advanced oxidation processes (AOPs) can remove organic matters effectively [11]. Some AOPs such as Fenton [12], Fenton-like system [13] and heterogeneous-like catalyst [14], which have recently been attracting great attention, have been used for pollutant degradation. In some

studies, a few environmentally friendly catalysts have been used for organic pollutant removal [15,16]. Mn_3O_4, as a practical oxidant, has magnetic, ion exchange, electrochemical and catalytic properties [17]. Many water-soluble catalysts are harmful to the environment whereas this is not the case for Mn_3O_4 because it can be recovered from water easily [18]. Moreover, it is an environmentally benign compound. It can even be more efficient in organic matter removal than iron nanoparticles. In the presence of this nanoparticle, $H_3K_5O_{18}S_4$ can create active SO_4^- radicals, which can treat effectively refractory materials, particularly PVA. It is a powerful oxidant (E^0 = 2.01) and is very stable under ordinary temperature (25°C) [19]. Furthermore, in the presence of Mn_3O_4 and H_2O_2, OH radicals are formed, which can mineralize a wide range of organic matters [14]. Some methods such as co-precipitation [20], thermal degradation [21], crystallization [22] and sol–gel [23] are used for preparing the Mn_3O_4 nanoparticles. Naturally, it has been a big challenge to introduce a way of having the fewest limitations like need to pressure and temperature control and using a detergent, as well as the coarser size of the produced particles making Mn_3O_4 difficult to be applied in the full-scale application. Therefore, in the present study, it was tried to synthesize the Mn_3O_4 nanoparticles through an easier measure under environmental conditions with higher efficiency. Also, the structural properties of the nanoparticles were studied and it was used as a catalyst in processes: Mn_3O_4/H_2O_2 and $Mn_3O_4/H_3K_5O_{18}S_4$ for PVA oxidation.

2. Materials and methods

2.1. Chemicals

All materials used in this study, including potassium permanganate (99%), hydrazine monohydrate (98%), pure ethanol, peroxymonosulfate (99%), hydrogen peroxide (30%), PVA (98%), boric acid (99.5%), potassium iodide (99.5%) and iodide (99.8%), were purchased from Merck Co. (Germany).

2.2. Synthesis and characterization of Mn_3O_4 nanoparticles

First, the Mn_3O_4 nanoparticle was synthesized through a co-precipitation method and the optical and structural properties of it were investigated. To this end, 4 mM of $KMnO_4$ was dissolved in 200 mL of distilled water on a magnetic mixer under environmental temperature (22°C). Next, 200 mL of hydrazine monohydrate solution containing 40 mM of hydrazine monohydrate was added quickly to the prepared solution on a mixer with a high rpm. At this stage, the color of the solution changed from violet to dark brown. The pH of the solution was adjusted at 9 by using H_2SO_4 (1 M). Then, the obtained solution was mixed for 15 min and finally was washed three times, twice with distilled water and once with ethanol and oven-dried at 50°C for 8 h [24]. To investigate the optical and structural properties of this nanoparticle, X-ray diffraction was used (Bruker D8 Advance, Germany). The surface area, pore-volume, and pore size were obtained using Brunauer–Emmett–Teller and Barrett–Joyner–Halenda (BELSORP-mini II, BEL Japan Inc.) methods, respectively. The field emission scanning electron microscope (FESEM; MIRA3TESCAN-XMU) was employed

to characterize the nanoparticles, by which the mesoporous structure of Mn_3O_4 was seen. Furthermore, Fourier transform infrared spectroscopy (Bruker Vertex 70 FTIR spectrometer; Germany) was used to characterize the immobilization of polyethylene glycol (PEG) and folic acid on the nanoparticle surfaces. To quantify the properties of the Mn_3O_4 nanoparticles, energy-dispersive X-ray spectroscopy was applied [25,26]. The results of all these analyses have been presented in detail in our previous study [27].

2.3. Experimental setup and procedure

All solutions in the present study were prepared synthetically. The stock solution (1,000 mg/L) was made as follows: 1 g of pure PVA was dissolved in 1 L of distilled water and other concentrations were prepared from the stock solution. To detect PVA contents, the absorbance of the test samples was determined via a UV-Vis spectrophotometer (HACH, DR5000; Germany) the maximum adsorbent wavelength of PVA (λ: 690 nm) [2,28,29]. All variables including pH (3, 5, 7, 9, and 11), $H_3K_5O_{18}S_4$ concentration (1.3, 2.6, 3.25, 3.9, and 4.88 mmol/L), H_2O_2 concentration (10, 20, 30, 40, and 50 mmol/L), Mn_3O_4 nanoparticle concentration (0.2, 0.3, 0.4, 0.5, and 0.6 g/L), contact time (20, 40, 60, 80, 100, and 120 min) and PVA concentration (25, 50, 100, 150, and 200 mg/L) were investigated in all steps in the current study. The experiments were conducted in two steps: the $Mn_3O_4/H_3K_5O_{18}S_4$ and Mn_3O_4/H_2O_2 processes and also the effects of the variables on the performance were studied.

3. Results and discussion

3.1. Effect of pH on PVA removal by Mn_3O_4/H_2O_2 and $Mn_3O_4/H_3K_5O_{18}S_4$ processes

Since in most AOPs reactions pH plays a direct role in OH radicals and, in turn, affects the performance, we first studied this parameter. To do this, three levels of pH (1) acidic conditions (pH 3 and 5), (2) neutral conditions (pH 7) and (3) alkaline conditions (pH 9 and 11) were examined. The results obtained have been shown in Figs. 1a and b. As can be seen, in the Mn_3O_4/H_2O_2 process, at pH = 3 and contact time = 120 min, the removal efficiency of PVA was 63.4%, but it decreased dramatically with increasing pH. And, in the case of $Mn_3O_4/H_3K_5O_{18}S_4$, at the same conditions, 88.84% and 62.4% of PVA were degraded at pHs = 3 and 11, respectively. Thus, the pH of 3 was selected as the optimum value for both methods and all other runs were conducted at this value. The reason for this decrease in performance with increasing pH value is the production of $HO_2^\bullet$ because of a reaction between $O_2^{\bullet-}$ and H^+. As a result, $HO_2^\bullet$ can form H_2O_2 that can be converted to $OH^\bullet$ [Eqs. (1)–(4)]. However, in alkaline conditions, hydroxyl radicals are quickly decomposed [30].

$$O_2^{\bullet-} + H^+ \rightarrow HO_2^\bullet \tag{1}$$

$$HO_2^\bullet + HO_2^\bullet \rightarrow H_2O_2 + O_2 \tag{2}$$

$$H_2O_2 + e^- \rightarrow HO^\bullet + OH^- \tag{3}$$
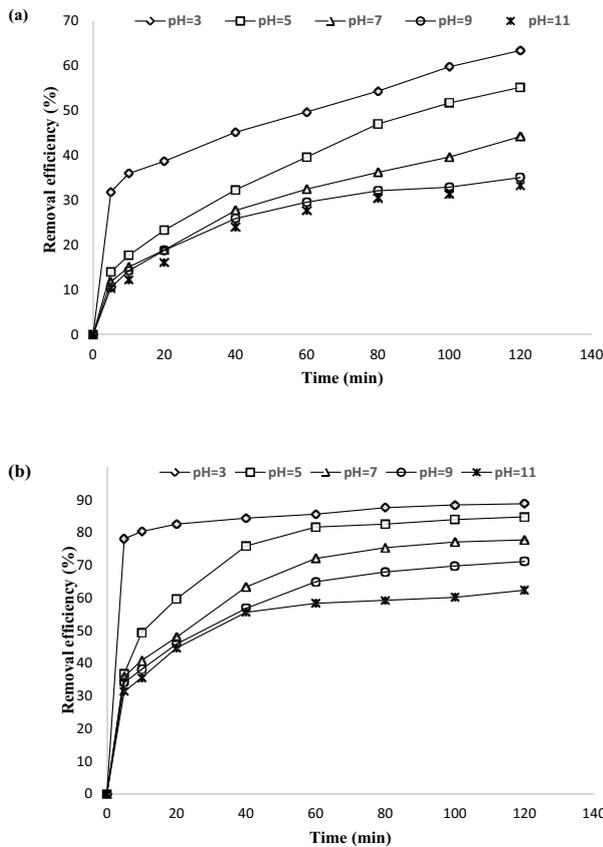
Fig. 1. Effect of solution pH on PVA removal (a) Mn_3O_4/H_2O_2 and (b) $Mn_3O_4/H_3K_5O_{18}S_4$ (PVA concentration = 100 mg/L, Mn_3O_4 = 0.4g/L, H_2O_2 = 20 mmol/L, $H_3K_5O_{18}S_4$ concentration = 3.25 mmol/L).

$$H_2O_2 + O_2^{•-} \rightarrow HO^• + OH^- + O_2 \tag{4}$$
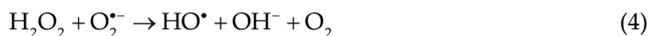
Also, in $Mn_3O_4/H_3K_5O_{18}S_4$, $SO_4^{•-}$ radical is converted to $OH^•$ under alkaline conditions [Eq. (5)]. The oxidation-reduction potential of hydroxyl radical declines with increasing pH, based on the above equations, thereby decreasing the production of $OH^•$, leading to a decline in the oxidation of the pollutant. Moreover, the radical of $SO_4^{•-}$ is relatively stable in acidic pHs and its active form is created in acidic conditions [31].

$$SO_4^{•-} + H_2O \rightarrow SO_4^{2-} + OH^• + H^+ \tag{5}$$

It should be pointed out that Lin et al. [28], who investigated the effect of the UV/S_2O_8 process on PVA removal from aqueous solutions, reported the similar observations; they claimed that pH played an important role in the process and the removal efficiency increased with declining pH. This decrease in performance is attributed to the reaction between sulfate radical and hydroxyl ion.

3.2. Effect of Mn_3O_4 nanoparticle concentration on PVA removal

In this work, different contents (0.2, 0.3, 0.4, 0.5, and 0.6 g/L) of the Mn_3O_4 nanoparticle were tested to study the
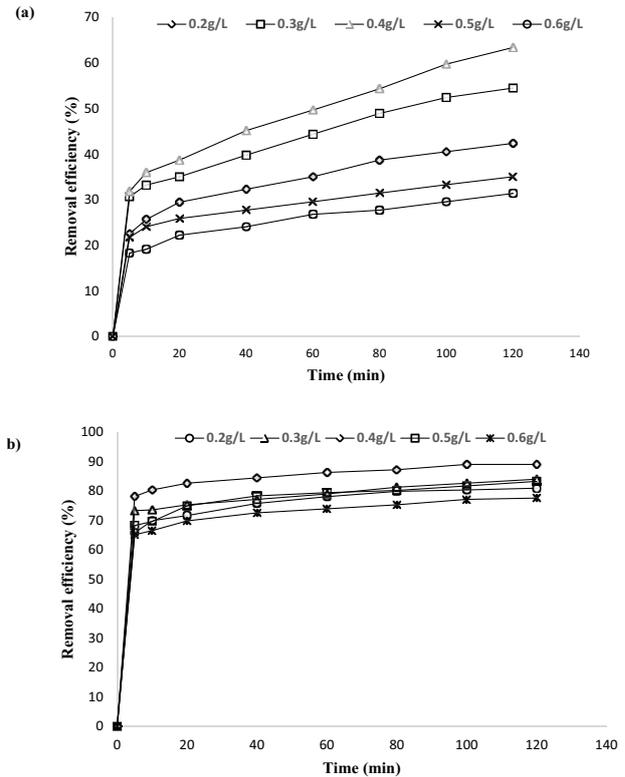
Fig. 2. Effect of initial dose of Mn_3O_4 on PVA removal (a) Mn_3O_4/H_2O_2 and (b) $Mn_3O_4/H_3K_5O_{18}S_4$ (PVA concentration = 100 mg/L, H_2O_2 = 20 mmol/L, $H_3K_5O_{18}S_4$ concentration = 3.25 mmol/L, pH = 3).

changes in the performance of the two methods; the findings have been shown in Figs. 2a and b. The removal efficiency increased with increasing the nanoparticle concentration up to 0.4 g/L and after this point, it decreased largely. As can be seen from the figure, the highest removal efficiencies were found to be 63.4% and 89.03%, respectively, for the processes of Mn_3O_4/H_2O_2 and $Mn_3O_4/H_3K_5O_{18}S_4$ at the PVA content of 100 mg/L and contact time of 120 min. This decrease in removal efficiency is attributed to the fact that at high concentrations of the nanoparticle the manganese ion, which is a basic agent in PVA oxidation, reacts with the hydroxyl ion and its concentration goes down. In the study by Saputra et al. [32], who compared the efficiency of the nanoparticles: Mn_3O_4, Fe_3O_4, and Co_3O_4 in phenol removal, it was shown that Mn_3O_4 had better performance and the removal efficiency went up when there was an increase in the concentration of the nanoparticle from 0.1 to 0.4 g/L; this observation is in agreement with those of the current research [32].

3.3. Effect of H_2O_2 concentration on PVA removal by Mn_3O_4/H_2O_2

We used the concentrations (10, 20, 30, 40, and 50 mmol/L) of H_2O_2 to determine changes in the removal efficiency of PVA. The highest removal efficiency (68.98%) was attained at the concentration of 20 mmol/L of H_2O_2 and 100 mg/L of PVA within 120 min, but it declined to 48.02% at the concentration of 50 mmol/L during 120 min (Fig. 3). In general, in the
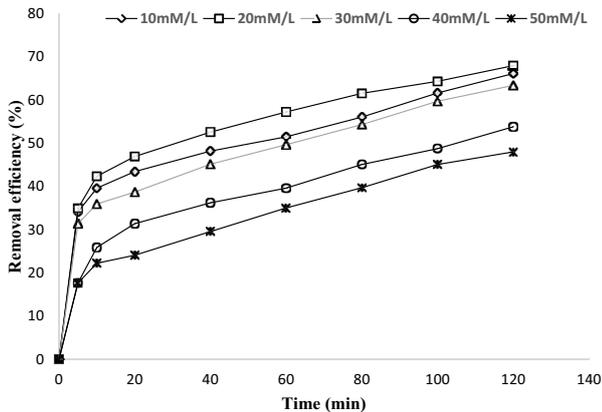
Fig. 3. Effect of initial hydrogen peroxide (H_2O_2) concentration on PVA removal by Mn_3O_4/H_2O_2 (PVA concentration = 100 mg/L, Mn_3O_4 concentration = 0.4 g/L, pH = 3).

Fig. 4. Effect of initial $H_3K_5O_{18}S_4$ concentration on PVA removal by $Mn_3O_4/H_3K_5O_{18}S_4$.

Mn_3O_4/H_2O_2 process, hydroxyl generated radicals by H_2O_2 and manganese tetroxide via three pathways including substitution with hydrogen, electron transfer or radical regeneration decompose the organic pollutant. Thus, it can be claimed that the more oxidant agent (H_2O_2), the more hydroxyl radical generation will be, which can further oxidize organic materials. As mentioned above, there was an increase in PVA removal with increasing H_2O_2 concentration, but with raising the content of H_2O_2 (higher than the optimum value), very lower amount of PVA was removed; at higher concentrations of H_2O_2, this oxidant acts as interference and consequently causes the removal efficiency to decrease because hydroxyl radical reacts with free H_2O_2 and is converted to H_2O and $HO_2^\bullet$. Besides, the produced $HO_2^\bullet$ reacts with hydroxyl radical and produces molecular oxygen; it should be noted that none of the produced materials has a noticeable oxidation power. This decrease in removal efficiency can be attributed to decreased H_2O_2 concentration against stable pollutant concentrations [33,34]. Zhang et al. [35] reported that, with increasing H_2O_2 concentration to 2.5 mmol/L, the removal efficiency of PVA increased and then declined dramatically; these observations accord those obtained in the current research. Moreover, in the study by Zhang et al. [36], who investigated the removal of PVA using ferrous and H_2O_2, it was found that the performance decreased from 52% to 10% with increasing the content of H_2O_2.

3.4. Effect of $H_3K_5O_{18}S_4$ concentration on PVA removal

In this study, the concentrations of 1.3, 2.6, 3.25, 3.9, and 4.88 mg/L of $H_3K_5O_{18}S_4$ were utilized to determine the change of the process performance at the initial PVA content of 100 mg/L (Fig. 4). As can be seen, with increasing the concentration of $H_3K_5O_{18}S_4$, the removal efficiency enhanced. It should be pointed out that this compound is a water-soluble oxidant and more stable than oxygen with the half-life of 10–20 d [37]. Under the ambient pressure, $H_3K_5O_{18}S_4$ does not affect highly organic materials, but, if heat, light or some special metal ions are used, its reactive power increases dramatically. According to the following equations, ionic
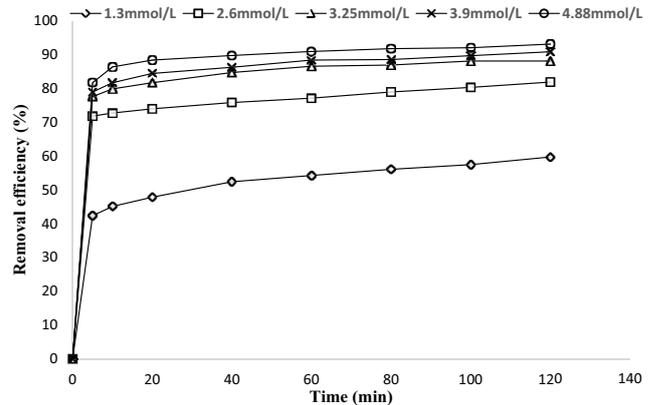
persulfate can be converted to H_2O_2 and sulfate ion in water, but H_2O_2 is quickly converted to water and oxygen [29].

$$HSO_5^- + 2Mn_3O_4 \rightarrow SO_4^{-\bullet} + H^+ + Mn_2O_3 \tag{6}$$

$$HSO_5^- + Mn_2O_3 \rightarrow SO_4^{-\bullet} + OH^- + 2Mn_3O_4 \tag{7}$$
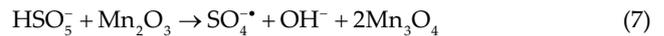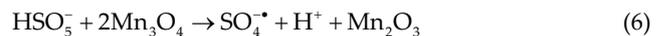
Recently, the activation of persulfate to form sulfate radicals and use them to treat and degraded organic materials have attracted great attention; some activation methods are as follows: the combination of persulfate with metal complexes, H_2O_2, alkaline persulfate, heat, light, ray and so on [37]. In the current research, Mn_3O_4 was used to activate persulfate. The findings showed that the performance of $Mn_3O_4/$ $H_3K_5O_{18}S_4$ in PVA removal increased with raising the concentration of $H_3K_5O_{18}S_4$ to 4.88 mmol/L within 120 min; this increase in removal efficiency is because of the generation of the radicals of sulfate and hydroxyl [38]. In accordance with our study, Saputra et al. [32], who worked on phenol removal by the nanoparticle of Mn_3O_4 and $H_3K_5O_{18}S_4$, documented that the efficiency improved with increasing $H_3K_5O_{18}S_4$ concentration [32].

3.5. Effect of initial PVA concentration on the processes of $Mn_3O_4/$ H_2O_2 and $Mn_3O_4/H_3K_5O_{18}S_4$

Different contents (25, 50, 100, 150, and 200 mg/L) of PVA were exerted to study changes of the removal efficiency under the following conditions: $H_3K_5O_{18}S_4$ concentration 4.88 mmol/L, nanoparticle concentration 0.4 g/L, H_2O_2 concentration 20 mmol/L and pH 3 (Figs. 5a and b). A decrease in PVA removal was observed with raising PVA content. This decrease in efficiency that happened through increasing pollutant content can be expressed by the kind of the contaminant and an AOP used in this study as in the processes of Mn_3O_4/H_2O_2 and $Mn_3O_4/H_3K_5O_{18}S_4$, only some certain amounts of active radicals are produced. Thus, these processes can oxidize and remove some specific levels of organic materials. The results of the study by Zhang et al. [35] showed a decline in removal efficiency via initial PVA concentration. Also, the impact of pollutant concentration on the removal efficiency of humic acid by the Fenton process was
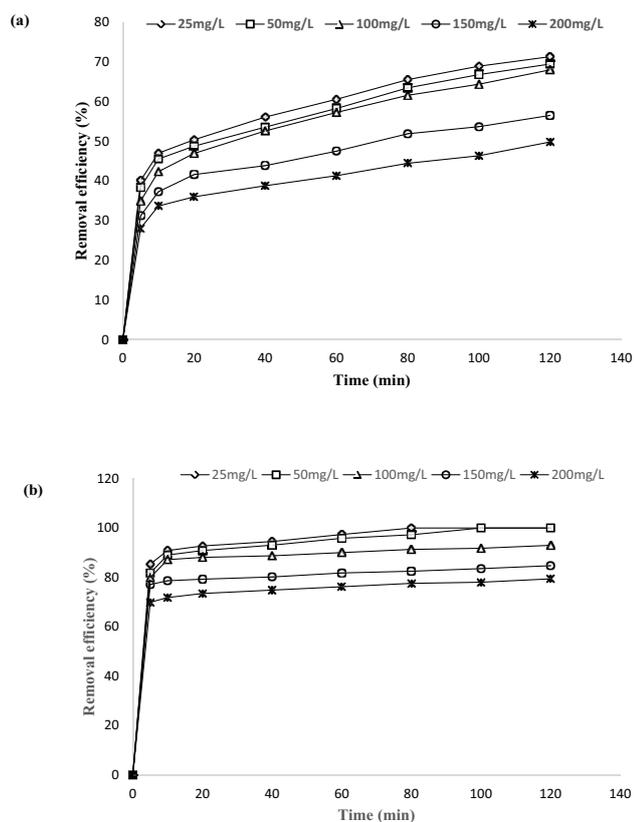
Fig. 5. Effect of initial PVA concentration on the removal efficiency (a) Mn_3O_4/H_2O_2 and (b) $Mn_3O_4/H_3K_5O_{18}S_4$.

Table 1
Kinetics (R^2) for the Mn_3O_4/H_2O_2 process

Concentration (mg/L)	Zero-order	First-order	Second-order
25	0.7709	0.9194	0.9583
50	0.7777	0.9047	0.9641
100	0.8023	0.9182	0.9701
150	0.7611	0.8622	0.9386
200	0.7434	0.8142	0.8988

Table 2
Kinetics (R^2) for the $Mn_3O_4/H_3K_5O_{18}S_4$ process

Concentration (mg/L)	Zero-order	First-order	Second-order
25	0.4407	0.6835	0.8646
50	0.4704	0.8898	0.8950
100	0.4084	0.6527	0.9167
150	0.3842	0.5118	0.7075
200	0.4153	0.5533	0.7304

studied. They reported that the performance of the process lessened substantially with raising the pollutant concentration because, at this stage, the number of the pollutant molecules increases while the concentration of hydroxyl radicals, which is dependent on the initial concentration of iron and hydrogen peroxide, is stable [39].

3.6. Kinetics of PVA degradation in $Mn_3O_4/H_3K_5O_{18}S_4$ and Mn_3O_4/H_2O_2

Tables 1 and 2 present the result of the kinetic of PVA degradation in the two processes. The findings illustrated that the two processes fit the second-order equation. Besides, we tested five levels of PVA concentration (25, 50, 100, 150, and 200 mg/L) to study the reaction rates; the results indicated that the R^2 coefficient increased with raising PVA content in both first- and second-order kinetics. Ertugay et al. [40] determined the kinetics of chemical oxygen demand (COD) removal via an AOP applied for dye removal; the results showed that the rate of the process in the second-order model showed the highest dependency. In the present study, the R^2 coefficient went up by increasing the concentration of the contaminant.

3.7. Synergistic effect of the key parameter of Mn_3O_4/H_2O_2 and $Mn_3O_4/H_3K_5O_{18}S_4$ processes and determination of COD removal

In order to investigate the synergistic impact of the variables influencing the Mn_3O_4/H_2O_2 and $Mn_3O_4/H_3K_5O_{18}S_4$ processes, some experiments were performed under the following conditions: initial PVA concentration = 100mg/L, pH = 3, H_2O_2 concentration = 20mmol/L, Mn_3O_4 concentration = 0.4 g/L, and $H_3K_5O_{18}S_4$ concentration = 4.88 mmol/L. As can be seen in Fig. 6, the highest removal efficiencies were attained in the processes of H_2O_2, Mn_3O_4, $H_3K_5O_{18}S_4$, Mn_3O_4/H_2O_2, and $H_3K_5O_{18}S_4$, which were 9.42%, 15.09%, 22.85%, 67.98%, and 92.96%, respectively. Since the mineralization of organic materials through processes like Mn_3O_4/H_2O_2 and $Mn_3O_4/H_3K_5O_{18}S_4$ or other methods is shown by a decrease in COD, at this stage, the performance of each method was measured via determining the level of COD removal. Therefore, some experiments under the following conditions: pH 3, PVA concentration 100 mg/L, Mn_3O_4 concentration 0.4 g/L, H_2O_2 concentration 20 mmol/L, and $H_3K_5O_{18}S_4$ concentration 4.88 mmol/L were conducted (Fig. 7). As can be seen, the rate of PVA removal was more than that of COD removal.

4. Conclusions

It was found that pH had a significant effect on the efficiency of the Mn_3O_4/H_2O_2 and $Mn_3O_4/H_3K_5O_{18}S_4$ processes and pH 3 showed the highest removal rates. Moreover, the removal efficiency of the two processes increased with increasing peroxymonosulfate and Mn_3O_4 concentration (up to 4.88 mmol/L and 0.4 g/L, respectively). Also, the maximum efficiency of Mn_3O_4/H_2O_2 was obtained at 20 mmol/L of hydrogen peroxide. Also, the efficiency of Mn_3O_4/H_2O_2 and $Mn_3O_4/H_3K_5O_{18}S_4$ processes decreased with increasing PVA concentration. The results of the kinetic study showed that the removal process followed the second-order kinetic for removing PVA in both processes.
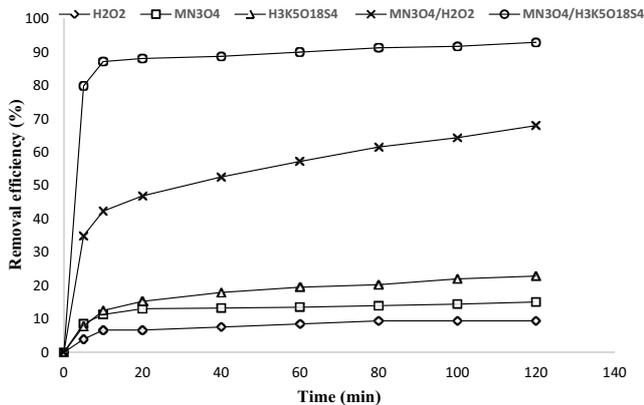
Fig. 6. Removal efficiency and synergistic effect of the PVA in various conditions in the aqueous solutions.
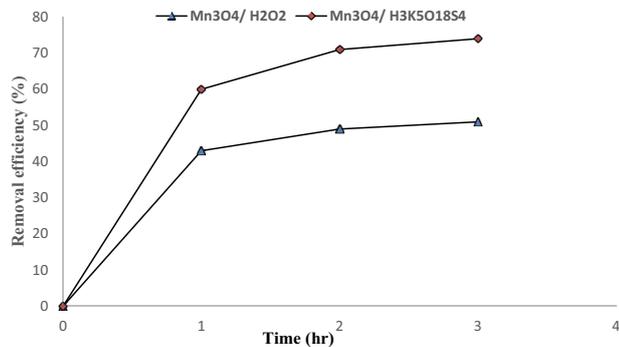
Fig. 7. Results of COD removal by Mn_3O_4/H_2O_2 and $Mn_3O_4/H_3K_5O_{18}S_4$.

Acknowledgment

References

[1] Y. Tokiwa, G. Kawabata, A. Jarerat, A modified method for isolating poly(vinyl alcohol)-degrading bacteria and study of their degradation patterns, Biotechnol. Lett., 23 (2001) 1937–1941.
[2] W.-L. Chou, C.-T. Wang, K.-Y. Huang, Investigation of process parameters for the removal of polyvinyl alcohol from aqueous solution by iron electrocoagulation, Desalination, 251 (2010) 12–19.
[3] Y.-t. Xiao, S.-s. Xu, Z.-h. Li, Degradation of polyvinyl-alcohol wastewater by Fenton's reagent: condition optimization and enhanced biodegradability, J. Cent. South. Univ. Technol., 18 (2011) 96–100.
[4] J. Giroto, R. Guardani, A. Teixeira, C. Nascimento, Study on the photo-Fenton degradation of polyvinyl alcohol in aqueous solution, Chem. Eng. Process., 45 (2006) 523–532.
[5] W.-L. Chou, C.-T. Wang, C.-W. Hsu, K.-Y. Huang, T.-C. Liu, Removal of total organic carbon from aqueous solution containing polyvinyl alcohol by electrocoagulation technology, Desalination, 259 (2010) 103–110.
[6] L.-J. Hsu, L.-T. Lee, C.-C. Lin, Adsorption and photocatalytic degradation of polyvinyl alcohol in aqueous solutions using P-25 TiO_2, Chem. Eng. Process., 173 (2011) 698–705.
[7] A.H. Mahvi, D. Naghipour, F. Vaezi, S. Nazmara, Teawaste as an adsorbent for heavy metal removal from industrial wastewaters, Am. J. Appl. Sci., 2 (2005) 372–375.
[8] J.-G. Lim, D.-H. Park, Degradation of polyvinyl alcohol by Brevibacillus laterosporus: metabolic pathway of polyvinyl alcohol to acetate, J. Microbiol. Biotechnol., 11 (2001) 928–933.
[9] S.K. Behera, J.-H. Kim, X. Guo, H.-S. Park, Adsorption equilibrium and kinetics of polyvinyl alcohol from aqueous solution on powdered activated carbon, J. Hazard. Mater., 153 (2008) 1207–1214.
[10] R. Solaro, A. Corti, E. Chiellini, Biodegradation of poly(vinyl alcohol) with different molecular weights and degree of hydrolysis, Polym. Adv. Technol., 11 (2000) 873–878.
[11] J.L. Wang, L.J. Xu, Advanced oxidation processes for wastewater treatment: formation of hydroxyl radical and application, Crit. Rev. Env. Sci. Technol., 42 (2012) 251–325.
[12] J. Tang, J. Wang, Metal organic framework with coordinatively unsaturated sites as efficient Fenton-like catalyst for enhanced degradation of sulfamethazine, Environ. Sci. Technol., 52 (2018) 5367–5377.
[13] Y. Liu, Q. Fan, J. Wang, Zn-Fe-CNTs catalytic in situ generation of H_2O_2 for Fenton-like degradation of sulfamethoxazole, J. Hazard. Mater., 342 (2018) 166–176.
[14] Z. Wan, J. Wang, Degradation of sulfamethazine using Fe_3O_4-Mn_3O_4/reduced graphene oxide hybrid as Fenton-like catalyst, J. Hazard. Mater., 324 (2017) 653–664.
[15] F. Ali, S.B. Khan, T. Kamal, K.A. Alamry, A.M. Asiri, Chitosan-titanium oxide fibers supported zero-valent nanoparticles: highly efficient and easily retrievable catalyst for the removal of organic pollutants, Sci. Rep., 8 (2018) 6260.
[16] F. Ali, S.B. Khan, T. Kamal, Y. Anwar, K.A. Alamry, A.M. Asiri, Anti-bacterial chitosan/zinc phthalocyanine fibers supported metallic and bimetallic nanoparticles for the removal of organic pollutants, Carbohydr. Polym., 173 (2017) 676–689.
[17] Y. Yamashita, K. Mukai, J. Yoshinobu, M. Lippmaa, T. Kinoshita, M. Kawasaki, Chemical nature of nanostructures of $La_{0.6}Sr_{0.4}MnO_3$ on $SrTiO_3$ (1 0 0), Surf. Sci., 514 (2002) 54–59.
[18] D.J. Cole-Hamilton, Homogeneous catalysis--new approaches to catalyst separation, recovery, and recycling, Science, 299 (2003) 1702–1706.
[19] S. Wang, J. Wang, Activation of peroxymonosulfate by sludge-derived biochar for the degradation of triclosan in water and wastewater, Chem. Eng. J., 356 (2019) 350–358.
[20] T. Ahmad, K.V. Ramanujachary, S.E. Lofland, A.K. Ganguli, Nanorods of manganese oxalate: a single source precursor to different manganese oxide nanoparticles (MnO, Mn_2O_3, Mn_3O_4), J. Mater. Chem., 14 (2004) 3406–3410.
[21] X. Sun, Y.W. Zhang, R. Si, C.H. Yan, Metal (Mn, Co, and Cu) oxide nanocrystals from simple formate precursors, Small, 1 (2005) 1081–1086.
[22] F. Jiao, A. Harrison, A.H. Hill, P.G. Bruce, Mesoporous Mn_2O_3 and Mn_3O_4 with crystalline walls, Adv. Mater., 19 (2007) 4063–4066.
[23] S. Lei, K. Tang, Z. Fang, H. Zheng, Ultrasonic-assisted synthesis of colloidal Mn_3O_4 nanoparticles at normal temperature and pressure, Cryst. Growth Des., 6 (2006) 1757–1760.
[24] P. Gibot, L. Laffont, Hydrophilic and hydrophobic nano-sized Mn_3O_4 particles, J. Solid State Chem., 180 (2007) 695–701.
[25] H. Jans, X. Liu, L. Austin, G. Maes, Q. Huo, Dynamic light scattering as a powerful tool for gold nanoparticle bioconjugation and biomolecular binding studies, Anal. Chem., 81 (2009) 9425–9432.
[26] K. Takahashi, H. Kato, T. Saito, S. Matsuyama, S. Kinugasa, Precise measurement of the size of nanoparticles by dynamic light scattering with uncertainty analysis, Part. Part. Syst. Char., 25 (2008) 31–38.
[27] R. Shokoohi, M.T. Samadi, G. Asgari, M.V. Tabar, K. Godini, Synthesis of manganese tetroxide nanoparticles using precipitation and study of its structure and optical characteristics, Avicenna J. Environ. Health Eng., 3 (2016), doi: 10.5812/ajehe.8565.

[28] C.-C. Lin, L.-T. Lee, L.-J. Hsu, Degradation of polyvinyl alcohol in aqueous solutions using UV-365 nm/$S_2O_8^{2-}$ process, Int. J. Environ. Sci. Technol., 11 (2014) 831–838.

[29] W.-L. Chou, L.-S. Chen, C.-T. Wang, S.-R. Lee, Electro-fenton removal of polyvinyl alcohol from aqueous solutions using an activated carbon fiber cathode, Fresenius Environ. Bull., 21 (2012) 3735–3742.

[30] S. Thongkrua, C. Ratanatamskul, Simultaneous removal of lignin and 2,4-dichlorophenol in pulp and paper mill wastewater using a supervibration-photocatalytic reactor, Mod. Appl. Sci., 5 (2011) 92.

[31] L. Hou, H. Zhang, X. Xue, Ultrasound enhanced heterogeneous activation of peroxydisulfate by magnetite catalyst for the degradation of tetracycline in water, Sep. Purif. Technol., 84 (2012) 147–152.

[32] E. Saputra, S. Muhammad, H. Sun, H.-M. Ang, M.O. Tadé, S. Wang, A comparative study of spinel structured Mn_3O_4, Co_3O_4 and Fe_3O_4 nanoparticles in catalytic oxidation of phenolic contaminants in aqueous solutions, J. Colloid Interface Sci., 407 (2013) 467–473.

[33] A. Babuponnusami, K. Muthukumar, Advanced oxidation of phenol: a comparison between Fenton, electro-Fenton, sono-electro-Fenton and photo-electro-Fenton processes, Chem. Eng. J., 183 (2012) 1–9.

[34] W.-P. Ting, M.-C. Lu, Y.-H. Huang, The reactor design and comparison of Fenton, electro-Fenton and photoelectro-Fenton processes for mineralization of benzene sulfonic acid (BSA), J. Hazard. Mater., 156 (2008) 421–427.

[35] S.-J. Zhang, H.-Q. Yu, Radiation-induced degradation of polyvinyl alcohol in aqueous solutions, Water Res., 38 (2004) 309–316.

[36] H. Zhang, L. Duan, Y. Zhang, F. Wu, The use of ultrasound to enhance the decolorization of the CI Acid Orange 7 by zero-valent iron, Dyes Pigm., 65 (2005) 39–43.

[37] P.A. Block, R.A. Brown, D. Robinson, Novel Activation Technologies for Sodium Persulfate in situ Chemical Oxidation, Proceedings of the Fourth International Conference on the Remediation of Chlorinated and Recalcitrant Compounds, Battelle Press, Columbus, OH, 2004, pp. 24–27.

[38] G. Asgari, A. Seidmohammadi, A. Chavoshani, Pentachlorophenol removal from aqueous solutions by microwave/persulfate and microwave/H_2O_2: a comparative kinetic study, J. Environ. Health Sci. Eng., 12 (2014) 94.

[39] Y. Wu, S. Zhou, F. Qin, K. Zheng, X. Ye, Modeling the oxidation kinetics of Fenton's process on the degradation of humic acid, J. Hazard. Mater., 179 (2010) 533–539.

[40] N. Ertugay, F.N. Acar, Removal of COD and color from Direct Blue 71 azo dye wastewater by Fenton's oxidation: kinetic study, Arab. J. Chem., 10 (2017) S1158–S1163.